



## 1 Tropospheric products of the 2<sup>nd</sup> European reprocessing (1996-2014)

2 Jan Dousa, Pavel Vaclavovic

3  
4 NTIS - New Technologies for the Information Society, Geodetic Observatory Pecný, RIGTC  
5 250 66 Zdíby, Czech Republic

6  
7 Correspondence to: J. Douša (jan.dousa@pecny.cz)

## 8 Abstract

9 In this paper, we present results of the 2<sup>nd</sup> reprocessing of all data from 1996 to 2014 from all  
10 stations in the European GNSS permanent network as performed at the Geodetic Observatory Pecný  
11 (GOP). While the original goal of this research was to ultimately contribute to new realization of the  
12 European terrestrial reference system, we also aim to provide a new set of GNSS tropospheric  
13 parameter time series with possible applications to climate research. To achieve these goals, we  
14 enhanced a strategy to guarantee the continuity of these tropospheric parameters and we prepared  
15 several variants of troposphere modelling. We then assessed all solutions in terms of the  
16 repeatability of coordinates as an internal evaluation of applied models and strategies, and in terms  
17 of zenith tropospheric delays (ZTD) and horizontal gradients with those of ERA-Interim numerical  
18 weather model (NWM) reanalysis. When compared to the GOP Repro1 solution, the results of the  
19 GOP Repro2 yielded improvements of approximately 50% and 25% in the repeatability of the  
20 horizontal and vertical components, respectively, and of approximately 9% in tropospheric  
21 parameters. Vertical repeatability was reduced from 4.14 mm to 3.73 mm when using the VMF1  
22 mapping function, a priori ZHD, and non-tidal atmospheric loading corrections from actual weather  
23 data. Raising the elevation angle cut-off from 3° to 7° and then to 10° increased RMS from  
24 coordinates' repeatability, which was then confirmed by independently assessing GNSS tropospheric  
25 parameters with the NWM reanalysis. The assessment of tropospheric horizontal gradients with  
26 respect to the ERA-Interim revealed a strong sensitivity of estimated gradients to the quality of GNSS  
27 antenna tracking performance. This impact was demonstrated at the Mallorca station, where  
28 gradients systematically grew up to 5 mm during the period between 2003 and 2008, before this  
29 behaviour disappeared when the antenna at the station was changed.

30 **Keywords:** GPS, reprocessing, zenith tropospheric delay, tropospheric horizontal gradients,  
31 coordinate time series, reference frame

## 32 1 Introduction

33 The US Global Positioning System (GPS) first became operational in 1995 as the first Global  
34 Navigation Satellite System (GNSS). Since that time, this technology has been transformed into a  
35 fundamental technique for positioning and navigation in everyday life. Hundreds of GPS permanent  
36 stations have been deployed for scientific purposes throughout Europe and the world, and the first  
37 stations have collected GPS data for approximately the last two decades. In 1994, a science-driven  
38 global network of continuously operating GPS stations was established by the International GNSS  
39 Service, IGS (<http://www.igs.org>) of the International Association of Geodesy (IAG) to support the  
40 determination of precise GPS/GNSS orbits and, clocks and earth rotation parameters, which are  
41 necessary for obtaining high-accuracy GNSS analyses for scientific applications. A similar network,



42 but regional in its scope, was also organized by the IAG Reference Frame Sub-Commission for Europe  
43 (EUREF) in 1996, which was called the EUREF Permanent Network (EPN), <http://epncb.oma.be>  
44 (Bruyninx et al. 2012). Although its primary purpose was to maintain the European Terrestrial  
45 Reference System (ETRS), the EPN also attempted to develop a pan-European infrastructure for  
46 scientific projects and co-operations (Ihde et al. 2014). Since 1996, the EPN has grown to include  
47 approximately 300 operating stations, which are regularly distributed throughout Europe and its  
48 surrounding areas. Today, EPN data are routinely analysed by 18 EUREF analysis centres.

49 Throughout the past two decades, GPS data analyses of both global and regional networks have been  
50 affected by various changes in processing strategy and updates of precise models and products,  
51 reference frames and software packages. To reduce discontinuities in products, particularly within  
52 coordinate time series, homogeneous reprocessing was initiated by the IGS and EUREF on a global  
53 and regional scale, respectively. To exploit the improvements in these IGS global products, the 2<sup>nd</sup>  
54 European reprocessing was performed in 2015-2016, with the ultimate goal of providing a newly  
55 realized ETRS.

56 Currently, station coordinate parameter time series from reprocessed solutions are mainly used in  
57 the solid earth sciences as well as to maintain global and regional terrestrial reference systems.  
58 Additionally, from an analytical perspective, the long-term series of estimated parameters and their  
59 residuals are useful for assessing the performances of applied models and strategies over a given  
60 period. Moreover, tropospheric parameters derived from this GNSS reanalysis could be useful for  
61 climate research (Yuan et al., 1993), due to their high temporal resolution and unrivalled relative  
62 accuracy for sensing water vapour when compared to other techniques, such as radio sounding,  
63 water vapour radiometers, and radio occultation (Ning, 2012). In this context, the GNSS Zenith  
64 Tropospheric Delay (ZTD) represents a site-specific parameter characterizing the total signal path  
65 delay in the zenith due to both dry (hydrostatic) and wet contributions of the neutral atmosphere,  
66 the latter of which is known to be proportional to precipitable water (Bevis et al. 1994).

67 With the 2<sup>nd</sup> EUREF reprocessing, the secondary goal of the GOP was to support the activity of  
68 Working Group 3 of the COST Action ES1206 (<http://gnss4swec.knmi.nl>), which addresses the  
69 evaluation of existing and future GNSS tropospheric products, and assesses their potential uses in  
70 climate research. For this purpose, GOP provided several solution variants, with a special focus on  
71 optimal tropospheric estimates, including VMF1 vs. GMF mapping functions, the use of different  
72 elevation cut-off angles, and estimates of tropospheric horizontal gradients using different time  
73 resolutions. Additionally, in order to enhance tropospheric outputs, we enhanced the processing  
74 strategy in a variety of ways compared to the GOP Repro1 solutions (Douša and Václavovic, 2012): 1)  
75 by combining tropospheric parameters in midnights and across GPS week breaks, 2) by checking  
76 weekly coordinates before their substitutions in order to estimate tropospheric parameters, and 3)  
77 by filtering out problematic stations by checking the consistency of daily coordinates. The results of  
78 this GOP reprocessing, including all available variants, were assessed using internal evaluations of  
79 applied models and strategy settings, and external validations with independent tropospheric  
80 parameters derived from numerical weather reanalyses.

81 In Section 2, we describe the processing strategy used in the 2<sup>nd</sup> GOP reanalysis of the EUREF  
82 permanent network. In Section 3, we describe the approach developed to guarantee continuity of  
83 estimated tropospheric parameters at midnights as well as between different GPS weeks. In Section



4, we present the results of internal and external evaluations of GOP solution variants and processing models. In Section 5, we present the relationship between mean tropospheric horizontal gradients and the quality of low-elevation GNSS tracking, which requires a more detailed study in the future. In the last section, we conclude our findings and suggest avenues of future research.

## 2 GOP processing strategy and solution variants

The EUREF GOP analysis centre was established in 1997, and contributed to operational EUREF analyses until 2013 by providing final, rapid, and near real-time solutions. Recently, GOP changed its contributions to that of a long-term homogeneous reprocessing of all data from the EPN historical archive. The GOP solution of the 1<sup>st</sup> EUREF reanalysis (Repro1) (Völksen, 2011) comprised the processing of a sub-network of 70 EPN stations during the period of 1996-2008. In 2011, for the first time, GOP reprocessed the entire EPN network (spanning a period of 1996-2010) in order to validate the European reference frame and to provide the first homogeneous time series of tropospheric parameters for all EPN stations (Douša and Václavovic, 2012).

In the 2<sup>nd</sup> EUREF reprocessing (Repro2), GOP analysed data obtained from the entire EPN network from a period of 1996-2014 using the Bernese GNSS Software V5.2 (Dach et al., 2015). As in the two previous GOP Repro1 solutions, this strategy relied on a network approach utilizing double-difference observations. GPS data from the EPN stations were included according to official validity intervals provided by the EPN central Bureau (<http://epncb.oma.be>). Two products were derived from the reprocessing campaign in order to contribute to a combination at the EUREF level performed by the coordinator of analysis centres and the coordinator of troposphere products: 1) site coordinates and corresponding variance-covariance information in daily and weekly SINEX files and 2) site tropospheric parameters in daily Tro-SINEX files.

This GOP processing was clustered into ten subnetworks (Figure 1) and then stacked into daily network solutions with pre-eliminated integer phase ambiguities. This strategy introduced state-of-the-art models (IERS Conventions, 2010) that are recommended as standards for highly accurate GNSS analyses, particularly for the maintenance of the reference frame. Additionally, the use of precise orbits obtained from the 2<sup>nd</sup> CODE global reprocessing (Dach et al., 2014) guaranteed complete consistency between all models on both the provider and user sides. Characteristics of this GOP data reprocessing strategy and their models are summarized in Table 1. Additionally, seven processing variants were performed during the GOP Repro2 analysis for studying selected models or settings: a) applying blind GMF (Böhm et al., 2006a) vs. actual VMF1 (Böhm et al., 2006b) tropospheric mapping functions, b) increasing the temporal resolution of tropospheric linear horizontal gradients in the north and east directions, c) using a different elevation angle cut-off, d) modelling atmospheric loading effects, and e) modelling higher-order ionospheric effects. Table 2 summarizes the settings and models of solution variants selected for generating coordinate and troposphere products, which are supplemented with variant rationales.

## 3 Ensuring ZTD continuity at midnights

When site tropospheric parameter time series generated from the EUREF 2<sup>nd</sup> reprocessing are applied to climate research, they should be free of artificial offsets in order to avoid misinterpretations (Bock and Willis, 2014). However, GNSS processing is commonly performed on a



124 daily basis according to adopted standards for data and product dissemination. Thus far, EUREF  
125 analysis centres have provided independent daily solutions, although precise IGS products are  
126 combined and distributed on a weekly basis. Station coordinates are estimated on a daily basis and  
127 are later combined to form more stable weekly solutions. According to the EUREF analysis centre  
128 guidelines ([http://www.epncb.oma.be/documentation/guidelines/guidelines\\_analysis\\_centres.pdf](http://www.epncb.oma.be/documentation/guidelines/guidelines_analysis_centres.pdf)),  
129 weekly coordinates should be used to estimate tropospheric parameters on a daily basis, but there  
130 are no requirements with which to guarantee the continuity of tropospheric parameters at  
131 midnights. Additionally, there are also discontinuities on a weekly basis, as neither daily coordinates  
132 nor hourly tropospheric parameters are combined across midnights between corresponding adjacent  
133 GPS weeks.

134 During the 1<sup>st</sup> GOP reprocessing, there was no way to guarantee tropospheric parameter continuity  
135 at midnight, as the troposphere was modelled by applying a piecewise constant model. In these  
136 cases, tropospheric parameters with a temporal resolution of one hour were reported in the middle  
137 of the hour, as was originally estimated. In the 2<sup>nd</sup> GOP reprocessing, using again hourly estimates,  
138 we applied a piecewise linear model for the tropospheric parameters. The parameter continuities at  
139 midnights were not guaranteed implicitly, but only by an explicit combination of parameters at daily  
140 boundaries. For the combination procedure we used three consecutive days while the tropospheric  
141 product stems from the middle day. The procedure is done again for three consecutive days shifted  
142 by one day. A similar procedure, using the piecewise constant model, was applied for estimating  
143 weekly coordinates which aimed to minimize remaining effects in consistency at transition of GPS  
144 weeks (at Saturday midnight). The coordinates of the weekly solution corresponding to the middle  
145 day of a three-day combination were fixed for the tropospheric parameter estimates. In the last step,  
146 we transformed the piecewise linear model to the piecewise constant model expressed in the middle  
147 of each hourly interval (HR:30), which was saved in the TRO-SINEX format to support the EUREF  
148 combination procedure requiring such sampling. The original piecewise linear parameter model was  
149 thus lost and to retain this information in the official product in the TRO-SINEX format, we  
150 additionally stored values for full hours (HR:00). Figure 2 summarizes four plots displaying  
151 tropospheric solutions with discontinuities in the left panels (a), (c) and enforcing tropospheric  
152 continuities in the right panels (b, d). While the upper plots (a), (b) display the piecewise constant  
153 model, bottom plots (c), (d) indicates the solution representing the piecewise linear model. The GOP  
154 Repro1 implementation is thus represented by Figure 2(a) plot while the GOP Repro2 solution  
155 corresponds to Figure 2(d).

156 These theoretical concepts were practically tested using a limited data set in 1996 (Figure 3). The  
157 panels in Figure 3 follow the organization of the theoretical plots shown in Figure 2; corresponding  
158 formal errors are also plotted along with estimated ZTDs. Discontinuities are visible in the left-hand  
159 plots and are usually accompanied by increasing formal errors for parameters close to data interval  
160 boundaries. As expected, discontinuities disappear in the right-hand plots. Although the values  
161 between 23:30 and 00:30 on two adjacent days are not connected by a line in the top-right plot,  
162 continuity was enforced for midnight parameters anyway, as seen in the bottom-right plot. Formal  
163 errors also became smooth near day boundaries, thus characterizing the contribution of data from  
164 both days and demonstrating that the concept behaves as expected in its practical implementation.



## 4 Assessment of reprocessing solutions

GOP variants and reprocessing models were assessed by a number of criteria, including those of the internal evaluations of coordinates' repeatability, residuals at reference stations, and the external validation of ZTDs and tropospheric horizontal gradients with data from numerical weather model (NWM) reanalyses.

### 4.1 Reference frame and station coordinates

We used coordinate repeatability to assess the quality of models applied in GNSS analysis. To be as thorough as possible, we not only assessed all GOP Repro2 variants but also assessed two GOP Repro1 solutions in order to discern improvements within the new reanalyses. The two Repro1 solutions differed in their used reference frames and PCV models: IGS05 and IGS08.

Table 3 summarizes mean coordinate repeatability in the North, East and Up components of all stations from their weekly combinations. All GOP Repro2 solution variants reached approximately 50% and 25% of the lower mean RMS of coordinate repeatability when compared to the GOP Repro1/IGS08 solution in its horizontal and vertical components, respectively. These values represent even greater improvements when compared to the GOP-Repro1/IGS05 solution. Comparing these two Repro1 solutions clearly demonstrates the beneficial impact of the new PCV models and reference frames. The observed differences between Repro2 and Repro1 also indicate an overall improvement of the processing software from V5.0 to V5.2, and the enhanced quality of global precise orbit and earth orientation products.

Various GOP Repro2 solutions were also used to assess the selected models. Variants GO0 and GO1 differ in their mapping functions (GMF vs VMF1) used to project ZTDs into slant path delays. These comparisons demonstrate that vertical component repeatability improved from 4.14 mm to 3.97 mm, whereas horizontal component repeatability decreased slightly. By increasing the elevation angle cut-off from 3° to 7° (GO2) and 10° (GO3), we observed a slight increase in RMS from repeatabilities of all coordinates. This can be explained by the positive impact of low-elevation observations on the decorrelation of height and tropospheric parameters, despite the fact that applied models (such as mapping functions, elevation-dependent weighting, PCVs, and multipath models) are still not optimal for including observations at very low elevation angles.

The GO4 solution represents an official GOP contribution to EUREF combined products. It is identical to the variant GO1, but applies a non-tidal atmospheric loading. We observed a positive improvement of approximately 9% for all coordinate components, which is less than the value of 20% previously observed on a global scale (Dach et al., 2011). No impact was observed on higher-order ionospheric effects (GO4 vs. GO5) from this coordinate repeatability, as the effects are systematic within the regional network (Fritsche et al., 2005), and were thus mostly eliminated by using reference stations in the domains of interest. The combination of tropospheric horizontal gradients with 6- to 24-hour resolution (GO4 vs. GO6) with the piece-wise linear model was also discovered to have a negligible impact on the coordinates' repeatability.

The terrestrial reference frame (Altamimi et al., 2001) is a realization of a geocentric system of coordinates used by space geodetic techniques. To avoid a degradation of GNSS products, differential GNSS analysis methods require a proper referencing of the solution to the system applied in the generation of precise GNSS orbit products. For this purpose we often use the concept of



fiducial stations with precise coordinates well-known in the requested system. Such stations are used to define the geodetic datum while their actual position can be re-adjusted by applying a condition minimizing coordinate residuals. None unique station is able to guarantee a stable monumentation and unchanged instrumentation during the whole reprocessing period. Thus a set of about 50 stations, with 100 and more time periods, was carefully prepared for GOP reprocessing and, for sufficient robustness, an iterative procedure of their validation was used for every processed day. Figure 4 then shows the evolution of the number of actually used fiducial stations (represented as red dots) from all configured fiducial sites (represented as black dots) after applying an iterative procedure of validation on a daily basis. This reprocessing began with the use of 16-20 fiducial stations, and this number increased to reach a maximum of over 50 during the period from 2003-2011. After 2011, this number decreased, due to a common loss of reference stations available from the last realization of the global terrestrial reference frame without changes in its instrumentation. In most cases, only 2 or 3 stations were excluded from the total number, however, this number is lower for some daily solutions, indicating the removal of even more stations. The lowest number of fiducial sites (12) was recorded on day 209 of the year 1999. We also observed seasonally variable, but rather consistent, mean RMS errors of horizontal, vertical, and total residuals of 6.47, 10.22, and 12.25 mm and 4.83, 7.94, 9.35 mm for daily and weekly solutions, respectively. These RMS errors demonstrate the stability of the reference system in the GOP reprocessing.

## 4.2 Tropospheric path delays and linear horizontal gradients

The EUREF tropospheric product comprises a combination of individual local analysis centre contributions, but includes only stations providing at least three contributions, in order to guarantee a robust product (Pacione et al., 2011). It is considered to be the most reliable and precise GNSS tropospheric product in Europe. Pacione et al. (2017) also demonstrated that, when assessed using independent data from the ERA-Interim reanalysis, it is apparent that the tropospheric parameters of the EUREF Repro2 outperform those of the Repro1 by 8–9%. This improvement is assumed to be even larger, as NWM quality is about twice as worse as that of the GNSS final products, and yield values of approximately 10 mm for NWM ZTD (Douša et al., 2016).

Initially, we compared all GOP Repro1 and Repro2 products to those of the EUREF-Repro1 combined solutions in terms of ZTD (Table 4), as the EUREF combination did not yet include tropospheric horizontal gradients. Table 4 demonstrates that ZTD reaches a level of 3 mm and exhibits a negligible common bias below 0.5 mm. The GOP-Repro1 thus demonstrates good agreement with the EUREF Repro1, as is expected based on its use of consistently precise products, processing models and Bernese software (V5.0). Similarly, we observe better agreement for the GO0 solution than for the GO1 solution, as the blind mapping function and a priori ZHD values are used in the cases of the GO0 and EUREF Repro1 analyses. Interestingly, we also observe increasing disagreement as the elevation angle cut-off increases, an observation that correlates with findings from the coordinate repeatability assessment. Additionally, we observe a significant reduction in RMS for the case in which the GO4 solution applies non-tidal atmospheric loading corrections along with an a priori ZHD model. These findings support those of Steigenberger et al. (2009), who demonstrated that modelling a priori ZHD values with mean, or slowly varying, empirical pressure values instead of true pressure values results in the partial compensation of atmospheric loading effects. We can observe this effect by comparing GO0, GO1 and GO4 variants. First, GO4 shows the best agreement with the old EUREF Repro1 combined solution, although both solutions use different models of mapping functions, a priori ZHD, and non-tidal atmospheric loading. Second, the GO1 variant performs worse than the GO0 variant,





250 although the actual mapping functions and ZHD a priori modelling outperform the blind models used  
 251 in the GO0 variant. This conclusion is also supported by the coordinate repeatability assessment from  
 252 the previous paragraphs and is confirmed through an independent assessment of ZTD, as is explained  
 253 in the following paragraphs.

254 We then compared reprocessed tropospheric parameters with respect to independent data from the  
 255 ERA-Interim global reanalysis (Dee et al. 2011), which were developed and provided by the European  
 256 Centre for Medium-Range Weather Forecasts (ECMWF) from 1969 to the present. For the period of  
 257 1996-2014, we calculated tropospheric parameters (namely ZTD and tropospheric horizontal linear  
 258 gradients) from the NWM for all EPN stations using the GFZ (German Research Centre for  
 259 Geosciences) ray-tracing software (Zus et al., 2014).

260 Table 5 displays comparisons of the GOP troposphere products with those obtained from the ERA-  
 261 Interim. This table shows that an overall ZTD bias reaches about -2 mm in all comparisons (GNSS –  
 262 NWM). However, this value is considered to be negligible when compared to the mean standard  
 263 deviation of the ZTD, which is approximately 8 mm. Comparing the results of the official GOP Repro2  
 264 solution (GO4) to those of the legacy solution (GO0) reveals an overall improvement of 9%, which is  
 265 similar to that of previous comparisons between the EUREF Repro1 and Repro2 products (Pacione et  
 266 al. 2016). Comparing the GO1 and GO0 variants demonstrates that the VMF1 mapping function  
 267 outperforms GMF if a low elevation angle of 3 degrees is used. These changes, as well as the decision  
 268 to use more accurate a priori ZHD, resulted in the ZTD standard deviation improving from 8.8 mm  
 269 (GO0) to 8.3 mm (GO1). Using non-tidal atmospheric loading corrections along with precise  
 270 modelling of a priori ZHD further contributed to this improvement by reducing this ZTD accuracy to  
 271 8.1 mm (GO4), which corresponds with the previous assessment of the coordinates' repeatability.  
 272 Similarly, ZTDs and tropospheric gradients recorded some degradation when the elevation angle cut-  
 273 off was raised from 3 degrees to 7 degrees (GO2) or 10 degrees (GO3). No impacts were observed  
 274 from modelling high-order ionospheric effects.

275 Comparing GO4 and GO6 solutions with those of an independent source revealed that standard  
 276 deviations dropped from 0.38 mm to 0.28 mm and from 0.40 mm to 0.29 mm for the East and North  
 277 gradients, respectively. The slightly worse performance of the GO4 solution is attributed to the fact  
 278 that tropospheric horizontal gradients were estimated with a 6-hour sampling interval and a piece-  
 279 wise linear function without the application of absolute or relative constraints. In such cases,  
 280 increased correlations of these gradients with other parameters can cause additional instabilities in  
 281 processing certain stations at specific times; these gradients can then absorb remaining errors in the  
 282 GNSS analysis model. The mean biases of the tropospheric gradients are considered to be negligible,  
 283 but we will demonstrate in the following section that some large systematic effects were indeed  
 284 discovered and were attributed to the quality of GNSS signal tracking.

285 Figure 5 also displays the time series of a long-term comparison of the GOP official ZTD product  
 286 (GO4) with respect to the results of the ERA-Interim reanalysis. The displayed mean bias and  
 287 standard deviation were derived from the monthly statistics of the GNSS-ERA differences.  
 288 Uncertainties of these mean values, represented by error bars, are derived from contributions from  
 289 all stations on a monthly basis. Generally, these time series show rather homogeneous results over  
 290 the given time span. The small observed increase in the mean standard deviation over time likely  
 291 reflects the increasing number of EPN sites established during the period, rising from approximately



292 30 to 300. The early years in this time series display a worse overall agreement in uncertainty values,  
 293 which can be attributed to the varying quality of historical observations and precise orbit products.  
 294 The mean bias varies from  $-3$  to  $1$  mm during this period, with a long-term mean of  $-1.8$  mm (Table  
 295 5). This long-term mean is relatively small compared to the recorded ZTD uncertainty of  
 296 approximately 5 mm.

297 Finally, Figure 6 displays the monthly time series comparing the GNSS and NWM tropospheric  
 298 horizontal gradients in both the North and East directions. Two solutions in particular are highlighted  
 299 in order to demonstrate the impact of different temporal resolutions; a 6-hour resolution is used for  
 300 GO4 and a 24-hour resolution is used for GO6. Error bars indicate the 1-sigma uncertainties of the  
 301 estimated monthly mean values. Although error bars are only displayed for the North gradients, they  
 302 are also considered to be representative of the East gradients. Values are plotted from zero on the y-  
 303 axis in order to better observe seasonal variations and trends. Seasonal variations are mainly  
 304 pronounced when observing estimates of mean standard deviations (top plot), whereas trends in  
 305 improvements are more pronounced for mean biases (bottom plot). Mean standard deviations and  
 306 their uncertainties (top plot) are lower by approximately 30% and 40%, respectively, within the 24-  
 307 hour resolution dataset of North and East tropospheric gradients (GO6) than they are in GO4; this  
 308 impact is especially pronounced in the early years of the dataset. These results indicate that  
 309 tropospheric gradients are highly correlated with other parameters, suggesting that careful handling  
 310 is needed in cases of applying sub-daily resolutions. Although it is not shown in the figure, the mean  
 311 standard deviations of the GO2 and GO3 solutions also increased by 8% and 12%, respectively, when  
 312 they used a higher elevation angle cut-off than the GO4 and GO6 solutions. However, no significant  
 313 differences in the mean biases of these North and East tropospheric gradients exist between these  
 314 solutions, although they share a common high variability during the years 1996-2001.

## 315 5 Relationship between tropospheric gradient biases and antenna 316 tracking

317 Using a new interactive web interface to conduct tropospheric parameter comparisons in the GOP-  
 318 TropDB (Györi and Douša, 2016), we observed large systematic tropospheric gradients during specific  
 319 years at several EPN stations. Generally, from GNSS data, we can only estimate total tropospheric  
 320 horizontal gradients without being able to distinguish between dry and wet contributions. The  
 321 former is mostly due to horizontal asymmetry in atmospheric pressure, and the latter is due to  
 322 asymmetry in the water vapour content. The latter is thus more variable in time and space than the  
 323 former (Li et al., 2015). Regardless, mean gradients should be close to zero, whereas dry gradients  
 324 may tend to point slightly more to the equator, corresponding to latitudinal changes in atmosphere  
 325 thickness (Meindl et al., 2004). Similarly, orography-triggered horizontal gradients can appear due to  
 326 the presence of high mountain ranges in the vicinity of the station (Morel et al., 2015). Such  
 327 systematic effects can reach the maximum sub-millimetre level, while a higher long-term gradient  
 328 (i.e.,  $>1$  mm), is likely more indicative of issues with site instrumentation, the environment, or  
 329 modelling effects. Therefore, in order to clearly identify these systematic effects, we also compared  
 330 our gradients with those calculated from the ERA-Interim.

331 It is beyond the scope of this paper to investigate in detail the correlation between tropospheric  
 332 horizontal gradients and antenna tracking performance. However, we do observe a strong impact in  
 333 the most extreme case identified when comparing gradients from the GNSS and the ERA-Interim for





all EPN stations. Figure 7 shows the monthly means of differences in the North and East tropospheric gradients from the MALL station (Mallorca, Spain). These differences increase from 0 mm up to -4 mm and 2 mm for the East and North gradients, respectively, within the period of 2003/06 - 2008/10. Such large monthly differences in GNSS and NWM gradients are not realistic, and were attributed to data processing when long-term increasing biases immediately dropped down to zero on November 1, 2008, immediately after the antenna and receiver were changed at the station.

The EPN Central Bureau (<http://epncb.oma.be>), operating at the Royal Observatory of Belgium (ROB), provides a web service for monitoring GNSS data quality and includes monthly snapshots of the tracking characteristics of all stations. The sequence of plots displayed in Figure 8, representing the interval of interest (2002, 2004, 2006 and 2008), reveals a slow but systematic and horizontally asymmetric degradation of the capability of the antenna to track low-elevation observations at the station. Therefore, we analysed days of the year (DoY) 302 and 306 (corresponding to October 28 and November 1, 2008) with the in-house G-Nut/Anubis software (Václavovic and Douša, 2016) and observed differences in the sky plots of these two days. The left-hand plot of Figure 9 depicts the severe loss of dual-frequency observations up to a 25-degree elevation angle in the South-East direction (with an azimuth of 90-180 degrees), which cause the tropospheric linear gradient of approximately 5 mm to point in the opposite direction. Figure 10 also demonstrates that an increasing loss of second frequency observations appears to occur in the East (represented as black dots). The right-hand plot in this figure demonstrates that both of these effects fully disappeared after the antenna was replaced on October 30, 2008 (DoY 304), resulting in the appearance of normal sky plot characteristics and a GLONASS constellation with one satellite providing only single frequency observations (represented as black lines).

This situation demonstrates the high sensitivity of the estimated gradients on data asymmetry, particularly at low-elevation angles. The systematic behaviour of these monthly mean gradients, their variations from independent data, and their profound progress over time seem to be useful indicators of instrumentation-related issues at permanent GNSS stations. These results can thus be used as useful tools for cleaning up GNSS historical archives, a necessary step before starting the 3<sup>rd</sup> EUREF reprocessing.

## 6 Conclusions

In this paper, we present results of the new GOP reanalysis of all stations within the EUREF Permanent network during the period of 1996-2014. This reanalysis was completed during the 2<sup>nd</sup> EUREF reprocessing to support the realization of a new European terrestrial reference system. In the 2<sup>nd</sup> reprocessing, we focused on analysing a new product – GNSS tropospheric parameter time-series for applications to climate research. To achieve this goal, we enhanced our strategy for combining tropospheric parameters at midnights and at transitions in GPS weeks. We also performed seven solution variants to study optimal troposphere modelling; we assessed each of these variants in terms of their coordinate repeatability by using internal evaluations of the applied models and strategies. We also compared tropospheric ZTD and tropospheric horizontal gradients with independent evaluations obtained by numerical weather reanalysis via the ERA-Interim.

Results of the GOP Repro2 yielded improvements of approximately 50% and 25% for their horizontal and vertical component repeatability, respectively, when compared to those of the GOP Repro1



375 solution. Vertical repeatability was reduced from 4.14 mm to 3.73 mm when using the VMF1  
 376 mapping function, a priori ZHD, and non-tidal atmospheric loading corrections from actual weather  
 377 data. Increasing the elevation angle cut-off from 3° to 7°/10° increased RMS errors of residuals from  
 378 these coordinates' repeatability. All of these factors were also confirmed by the independent  
 379 assessment of tropospheric parameters using NWM reanalysis data.

380 We particularly recommend using low-elevation observations along with the VMF1 mapping  
 381 function, as well as using precise a priori ZHD values with the consistent model of non-tidal  
 382 atmospheric loading. While estimating tropospheric horizontal linear gradients improves  
 383 coordinates' repeatability, 6-hour sampling without any absolute or relative constraints revealed a  
 384 loss of stability due to its correlations with other parameters. Finally, assessing the tropospheric  
 385 horizontal gradients with respect to the ERA-Interim reanalysis data revealed some long-term  
 386 systematic behaviour linked to degradation in antenna tracking quality. We presented an extreme  
 387 case at the Mallorca station (MALL), in which gradients systematically increased up to 5 mm from  
 388 2003-2008 while pointing in the direction of prevailing observations at low elevation angles.  
 389 However, these biases disappeared when the malfunctioning antenna was replaced. More cases  
 390 similar to this, although less extreme, have indicated that estimated tropospheric gradients are  
 391 extremely sensitive to the quality of GNSS antenna tracking, thus suggesting that these gradients can  
 392 be used to identify problems with GNSS data tracking in historical archives.

393 One of the main difficulties faced during the 2<sup>nd</sup> reprocessing was that of the quality of the historical  
 394 data, which contains a large variety of problems. We removed data that caused significant problems  
 395 in network processing when these could not be pre-eliminated from normal equations during the  
 396 combination process without still affecting daily solutions. To provide high-accuracy, high-resolution  
 397 GNSS tropospheric products, the elimination of such problematic data or stations is even more  
 398 critical considering the targeting static coordinates on a daily or weekly basis for the maintenance of  
 399 the reference frame or the derivation of a velocity field. Before undertaking the 3<sup>rd</sup> EUREF  
 400 reprocessing, which is expected to begin after significant improvements have been made to state-of-  
 401 the-art models, products and software, we need to improve data quality control and clean the EUREF  
 402 historical archive in order to optimize any future reprocessing efforts and to increase the quality of  
 403 tropospheric products. These efforts should also include the collection and documentation of all  
 404 available information from each step of the 2<sup>nd</sup> EUREF reprocessing, including individual  
 405 contributions, EUREF combinations, time-series analyses and coordinates, and independent  
 406 evaluations of tropospheric parameters.

## 407 Acknowledgments

408 The reprocessing effort and its evaluations were supported by the Ministry of Education, Youth and  
 409 Science, the Czech Republic (projects LD14102 and LO1506).

## 410 References

- 411 • Altamimi, Z., Angermann, D., Argus, D., et al.: The terrestrial reference frame and the  
 412 dynamic Earth, EOS, Transactions, American Geophysical Union, 82, 273–279, 2001.



- 1413 • Bevis, M., Businger, S., Chiswell, S., Herring, T. A., Anthes, R. A., Rocken C, and Ware R. H.:  
1414 GPS Meteorology: Mapping Zenith Wet Delays onto Precipitable Water, *J. Appl. Meteorol.*,  
1415 33, 379–386, 1994.
- 1416 • Bock, O., Willis, P., Wang, J., and Mears, C.: A high-quality, homogenized, global, long-term  
1417 (1993–2008) DORIS precipitable water data set for climate monitoring and model  
1418 verification, *J. Geophys. Res. Atmosphere*, 119, 7209–7230, 2014.
- 1419 • Böhm, J., Niell, A.E., Tregoning, P., and Schuh, H.: 2006, Global Mapping Functions (GMF): A  
1420 new empirical mapping function based on numerical weather model data, *Geophys. Res.*  
1421 *Lett.*, 33, L07304, 2006a.
- 1422 • Böhm, J., Werl, B., and Schuh, H.: Troposphere mapping functions for GPS and very long  
1423 baseline interferometry from European Centre for Medium-Range Weather Forecasts  
1424 operational analysis data. *J. Geophys. Res.*, 111, B02406, 2006b.
- 1425 • Bruyninx, C., Habrich, H., Söhne, W., Kenyeres, A., Stangl, G., Völksen, C.: Enhancement of the  
1426 EUREF Permanent Network Services and Products, *Geodesy for Planet Earth*, IAG Symposia  
1427 Series, 136, 27–35, 2012.
- 1428 • Dach, R., Böhm, J., Lutz, S., Steigenberger, P. and Beutler, G.: Evaluation of the impact of  
1429 atmospheric pressure loading modeling on GNSS data analysis, *J. Geod.*, 85(2), 75–91, 2011.
- 1430 • Dach, R., Schaer, S., Lutz, S., Baumann, C., Bock, H., Orliac, E., Prange, L., Thaller, D., Mervart,  
1431 L., Jäggi, A., Beutler, G., Brockmann, E., Ineichen, D., Wiget, A., Weber, G., Habrich, H., Söhne,  
1432 W., Ihde, J., Steigenberger, P., and Hugentobler, U.: CODE IGS Analysis Center Technical  
1433 Report 2013, Dach, R., and Jean, Y. (eds.), IGS 2013 Tech. Rep., 21–34, 2014.
- 1434 • Dach, R., Lutz, S., Walser, P., Fridez, P. (Eds.): *Bernese GNSS Software Version 5.2. User*  
1435 *manual*, Astronomical Institute, University of Bern, Bern Open Publishing, 2015.
- 1436 • Dee, D.P., Uppala, S.M., Simmons, A.J. et al.: The ERA-Interim reanalysis: Configuration and  
1437 performance of the data assimilation system, *Q. J. Roy. Meteorol. Soc.*, 137, 553–597, 2011.
- 1438 • Douša, J., Václavovic, P.: Results of GPS Reprocessing campaign (1996–2011) provided by  
1439 Geodetic observatory Pecný, *Geoinformatics, FCE CTU*, 9, 77–89, 2012.
- 1440 • Douša, J., Dick, G., Kačmařík, M., Brožková, R., Zus, F., Brenot, H., Stoycheva, A., Möller, G.,  
1441 and Kaplon, J.: Benchmark campaign and case study episode in central Europe for  
1442 development and assessment of advanced GNSS tropospheric models and products, *Atmos.*  
1443 *Meas. Tech.*, 9, 2989–3008, 2016.
- 1444 • Fritsche, M., Dietrich, R., Knofel, C., Rülke, A., Vey, S., Rothacher, M., Steigenberger, P.:  
1445 Impact of higher-order ionospheric terms on GPS estimates. *Geophys. Res. Lett.*, 32, L23311,  
1446 2005.
- 1447 • Györi, G., Douša, J.: GOP-TropDB developments for tropospheric product evaluation and  
1448 monitoring – design, functionality and initial results, *IAG Symposia Series*, Springer, 143, 595–  
1449 602, 2016.
- 1450 • Ihde, J., Habrich, H., Sacher, M., Söhne, W., Altamimi, Z., Brockmann, E., Bruyninx, C.,  
1451 Caporali, A., Dousa, J., Fernandes, R., Hornik, H., Kenyeres, A., Lidberg, M., Makinen, J.,  
1452 Poutanen, M., Stangl, G., Torres, J.A., Völksen, C.: EUREF's Contribution to National,  
1453 European and Global Geodetic Infrastructures, In: *Earth on the Edge: Science for a*  
1454 *Sustainable Planet*, Rizos, C. and Willis P. (eds), IAG Symposia Series, Springer, 139, 189–196,  
1455 2014.



- 456 • IERS Conventions: Gérard, P., and Luzum, B. (Eds.), IERS Technical Note No. 36, Frankfurt am  
457 Main: Verlag des Bundesamts für Kartographie und Geodäsie, 179 pp., 2010.
- 458 • Li, X., Zus, F., Lu, C., Ning, T., Dick, G., Ge, M., Wickert, J., and Schuh, H.: Retrieving high-  
459 resolution tropospheric gradients from multiconstellation GNSS observations, *Geophys. Res.*  
460 *Lett.*, 42(10), 4173–4181, 2015.
- 461 • Meindl, M., Schaer, S., Hugentobler, U., and Beutler, G.: Tropospheric Gradient Estimation at  
462 CODE: Results from Global Solutions. *Journal of the Meteorological Society of Japan*, 82,  
463 331–338, 2004.
- 464 • Morel, L., Pottiaux, E., Durand, F., Fund, F., Follin, J.M., Durand, S., Bonifac, K., Oliveira, P.S.,  
465 van Baelen, J., Montibert, C., Cavallo, T., Escaffit, R., and Fragnol, L.: Global validity and  
466 behaviour of tropospheric gradients estimated by GPS, presentation at the 2<sup>nd</sup> GNSS4SWEC  
467 Workshop held in Thessaloniki, Greece, May 11-14, 2015.
- 468 • Ning, T.: GPS Meteorology: With Focus on Climate Applications, PhD Thesis, Dept. Earth and  
469 Space Sciences. Chalmers University of Technology, 2012.
- 470 • Pacione, R., Pace, B., de Haan, S., Vedel, H., Lanotte, R., Vespe, F.: Combination Methods of  
471 Tropospheric Time Series, *Adv. Space Res.*, 47, 323–335, 2011.
- 472 • Pacione, R., Araszkiewicz, A., Brockmann, E., Douša, J.: EPN Repro2: A reference GNSS  
473 tropospheric dataset over Europe, submitted to *Atmosph. Meas. Tech.*, 2017
- 474 • Steigenberger, P., Böhm, J., Tesmer, V.: Comparison of GMF/GPT with VMF1/ECMWF and  
475 implications for atmospheric loading, *J. Geod.*, 83, 943, 2009.
- 476 • Václavovic, P., Douša, J.: G-Nut/Anubis - open-source tool for multi-GNSS data monitoring, In:  
477 IAG 150 Years, Rizos, Ch. and Willis, P. (eds), IAG Symposia Series, Springer, 143, 775-782,  
478 2016.
- 479 • Völksen, C.: An update on the EPN Reprocessing Project: Current Achievements and Status,  
480 Presented at the EUREF 2011 Symposium, Chisinau, Republic of Moldova, May 25-28.  
481 [http://www.epncb.oma.be/\\_documentation/papers/eurefsymposium2011/an\\_update\\_on\\_e](http://www.epncb.oma.be/_documentation/papers/eurefsymposium2011/an_update_on_e)  
482 [pn\\_reprocessing\\_project\\_current\\_achievement\\_and\\_status](http://www.epncb.oma.be/_documentation/papers/eurefsymposium2011/an_update_on_e), 2011
- 483 • Yuan, L.L., Anthes, R.A., Ware, R.H., Rocken, C., Bonner, W.D., Bevis, M.G., and Businger, S.:  
484 Sensing Climate Change Using the Global Positioning System, *J. Geophys. Res.*, 98, 14925–  
485 14937, 1993.
- 486 • Zus, F., Dick, G., Heise, S., Dousa, J., and Wickert, J.: The rapid and precise computation of  
487 GPS slant total delays and mapping factors utilizing a numerical weather model, *Radio Sci.*,  
488 49, 207–216, 2014.
- 489



490 **Table 1: Characteristics of GOP reprocessing models**

Processing options	Description
Products	CODE precise orbit and earth rotation parameters from the 2 <sup>nd</sup> reprocessing.
Observations	Dual-frequency code and phase GPS observations from L1 and L2 carriers. Elevation cut-off angle 3 degree, elevation-dependent weighting $1/\cos^2$ (zenith), double-difference observations and with 3-minute sampling rate.
Reference frame	IGb08 realization, core stations set as fiducial after a consistency checking. Coordinates estimated using a minimum constraint.
Antenna model	GOP: IGS08_1832 model (receiver and satellite phase centre offsets and variations).
Troposphere	A priori zenith hydrostatic delay of VMF1/Saastamoinen model and VMF1/GMF mapping function. Estimated ZTD corrections every hour using VMF1 wet mapping function; 5 m and 1 m for absolute and relative constraints, respectively. Estimated horizontal NS and EW tropospheric gradients every 6 hours with no a priori tropospheric gradients and very loose absolute/relative constraints.
Ionosphere	Eliminated using ionosphere-free linear combination with applying higher-order effects estimated using CODE global ionosphere product.
Loading effects	Atmospheric tidal loading and hydrology loading not applied. Ocean tidal loading FES2004 used. Non-tidal atmospheric loading introduced in advanced variants from the model from TU-Vienna.

491



492 **Table 2: GOP solution variants for the assessment of selected models and settings**

Solution ID	Specific settings and differences	Remarks and rationales
GO0	GMF and 3° cut-off	Legacy solution for Repro1
GO1	VMF1 and 3° cut-off	New candidate for Repro2
GO2	=GO1; 7° cut-off	Impact of elevation degree cut-off
GO3	=GO1; 10° cut-off	Impact of elevation degree cut-off
GO4	=GO1; atmospheric loading	Non-tidal atmospheric loading applied
GO5	=GO4; higher-order ionosphere	Higher-order ionosphere effect not applied
GO6	=GO4; 24-hour gradients	Stacking tropospheric gradients to 24-hour sampling

493





494

**Table 3: Comparison of GOP solution variants for North, East and Up coordinate repeatability.**

Solution	North RMS [mm]	East RMS [mm]	Up RMS [mm]
GOP-Repro1/IGS05	3.01	2.40	5.08
GOP-Repro1/IGS08	2.64	2.21	4.94
GO0	1.20	1.30	4.14
GO1	1.23	1.33	3.97
GO2	1.24	1.33	4.01
GO3	1.26	1.34	4.07
GO4	1.14	1.24	3.73
GO5	1.14	1.24	3.73
GO6	1.14	1.24	3.73

495



496

**Table 4: GOP reprocessing ZTDs compared to EUREF Repro1 products**

Solution	ZTD BIAS [mm]	ZTD SDEV [mm]	ZTD RMS [mm]
GOP-Repro1	0.39	2.18	2.25
GO0	0.88	2.82	3.06
GO1	0.39	2.98	3.15
GO2	0.48	3.18	3.34
GO3	0.49	3.35	3.51
GO4	0.45	2.52	2.62
GO5	0.40	2.52	2.62
GO6	0.41	2.58	2.71

497



498 **Table 5: Statistics (bias and standard deviations) of ZTD and tropospheric gradients from the seven reprocessing variants**  
 499 **compared to those obtained from the ERA-Interim NWM reanalysis.**

Solution	ZTD [mm]	E-gradient [mm]	N-gradient [mm]
	Bias ± Sdev	Bias ± Sdev	Bias ± Sdev
GO0	-1.5 ± 8.8	-0.04 ± 0.39	+0.01 ± 0.43
GO1	-2.0 ± 8.3	-0.04 ± 0.39	+0.01 ± 0.42
GO2	-1.9 ± 8.4	-0.05 ± 0.41	+0.00 ± 0.45
GO3	-1.8 ± 8.5	-0.08 ± 0.43	-0.01 ± 0.49
GO4	-1.8 ± 8.1	-0.04 ± 0.38	+0.00 ± 0.40
GO5	-1.8 ± 8.1	-0.05 ± 0.38	+0.01 ± 0.40
GO6	-1.8 ± 8.2	-0.04 ± 0.29	+0.01 ± 0.28

500

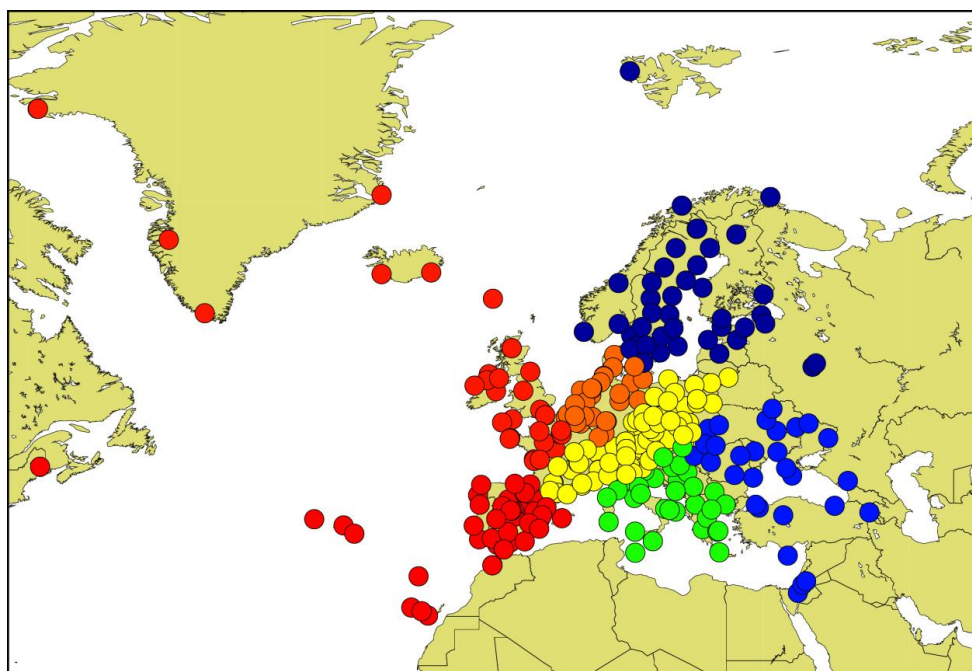
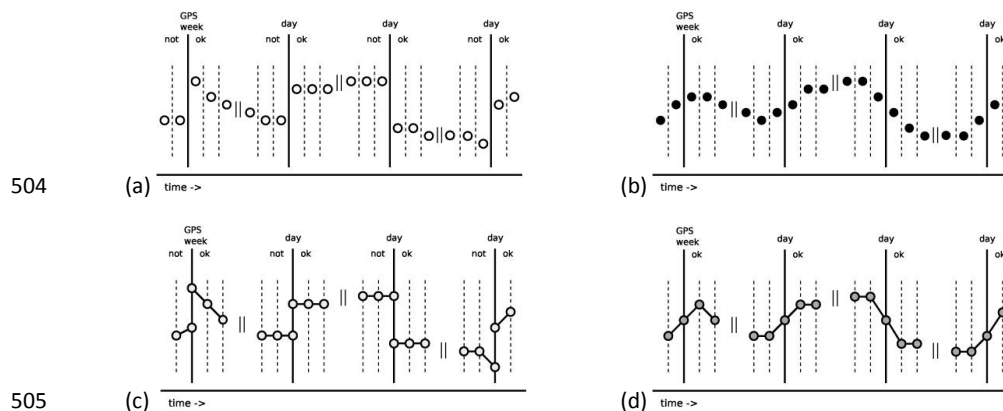
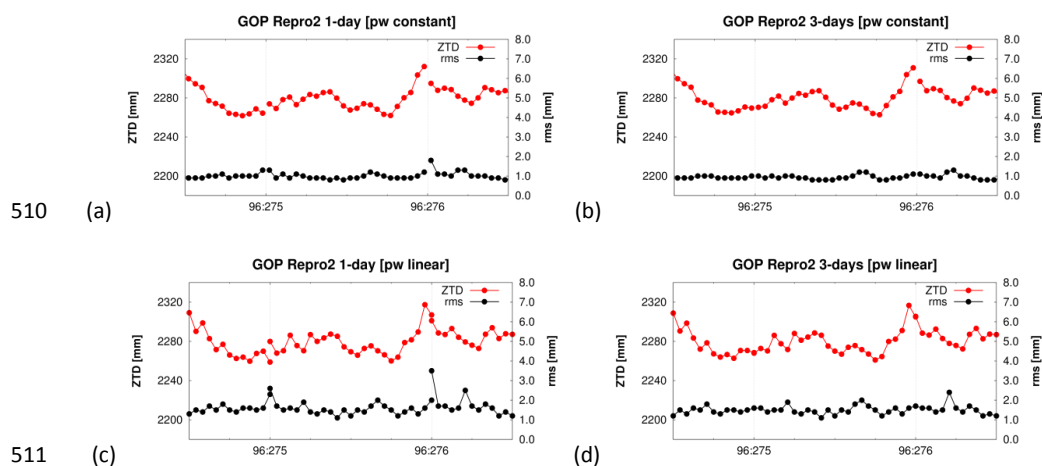


Figure 1: EUREF Permanent Network's clusters (designated by different colours) in the 2<sup>nd</sup> GOP reprocessing.

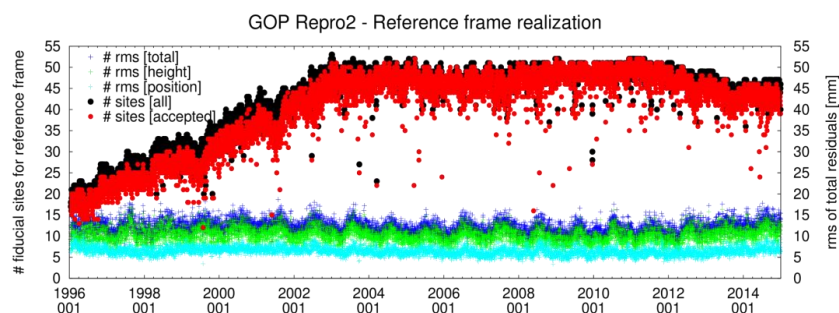


**Figure 2: Charts of 4 variations on representations of tropospheric parameters. Right (b), (d) and left (a), (c) panels display estimates made with and without midnight combinations, respectively. Top (a), (b) and bottom (c), (d) panels display the piecewise constant and the linear model, respectively.**



**Figure 3: Four variations in representation of tropospheric parameters. Right (b), (d) and left (a), (c) panels display estimates with and without midnight combinations, respectively. Top (a), (b) and bottom (c), (d) panels display the piecewise constant and the piecewise linear model, respectively.**





516

517 **Figure 4: Statistics of the daily reference system realization: a) RMS of residuals at fiducial stations (representing the**  
 518 **total, height and position); b) number of stations (all and accepted after an iterative control)**

519

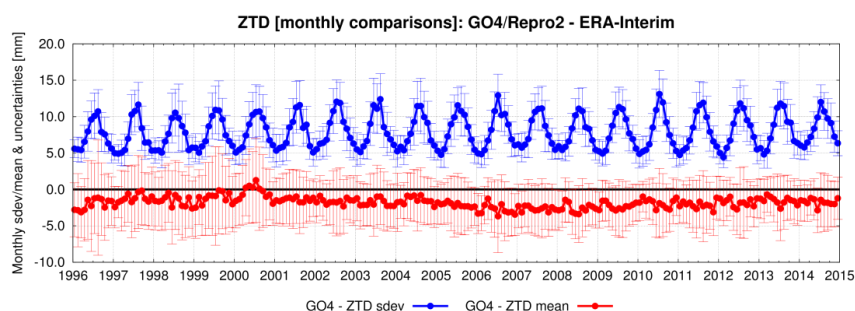


Figure 5: Monthly means of bias and standard deviation of official GOP ZTD product compared to those of the ERA-Interim.

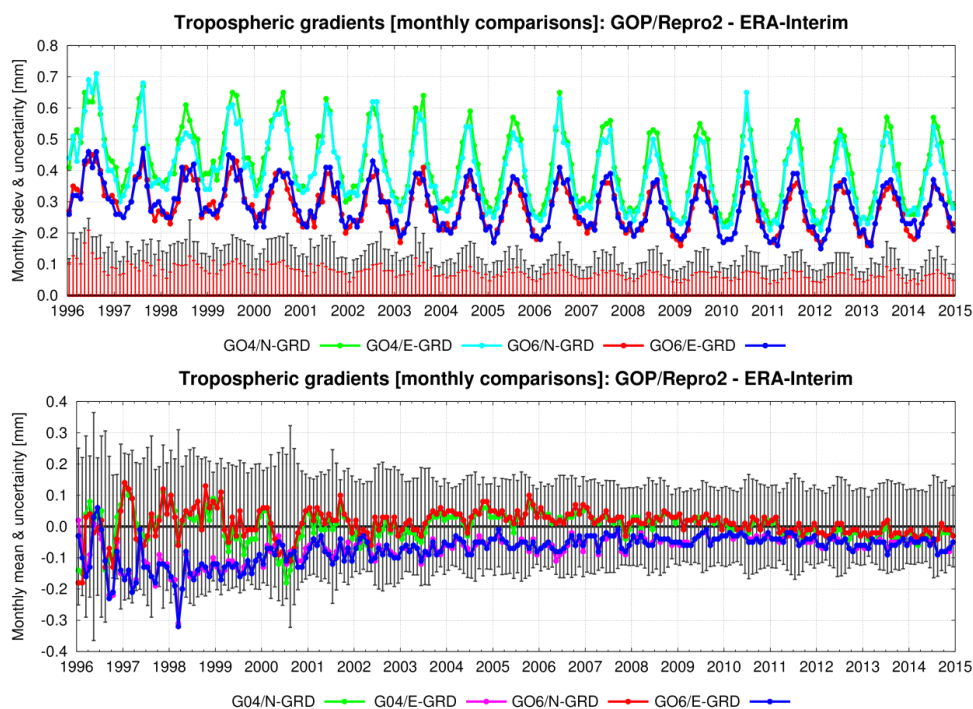


Figure 6: Monthly means of bias and standard deviation of tropospheric horizontal North (N-GRD) and East (E-GRD) gradients compared to those obtained by ERA-Interim. Note: Similar products are almost superposed.

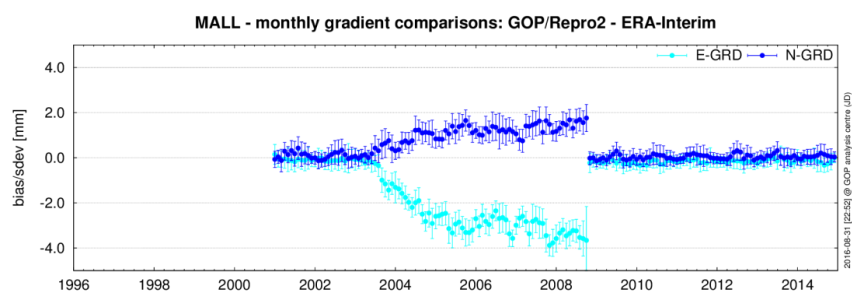
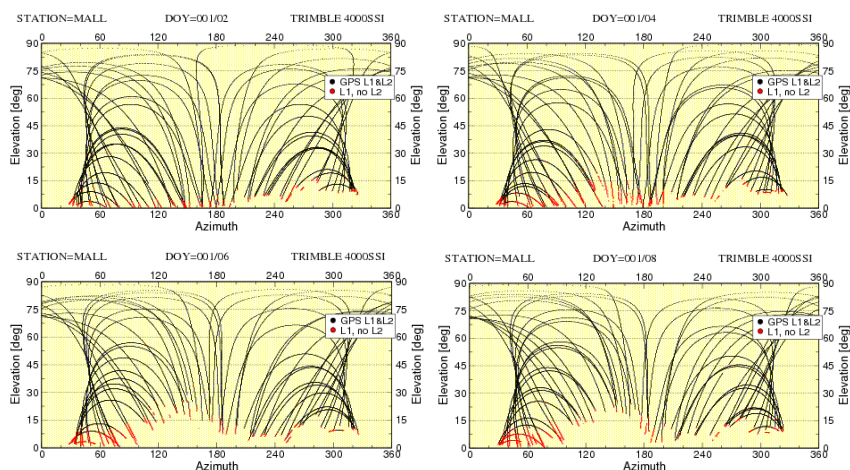


Figure 7: MALL station - monthly mean differences in tropospheric horizontal gradients with respect to the ERA-Interim.



**Figure 8: Low-elevation tracking problems at the MALL station during the period of 2003-2008. From left-to right-bottom: January 2002, 2004, 2006 and 2008 (courtesy of the EPN CB, ROB).**

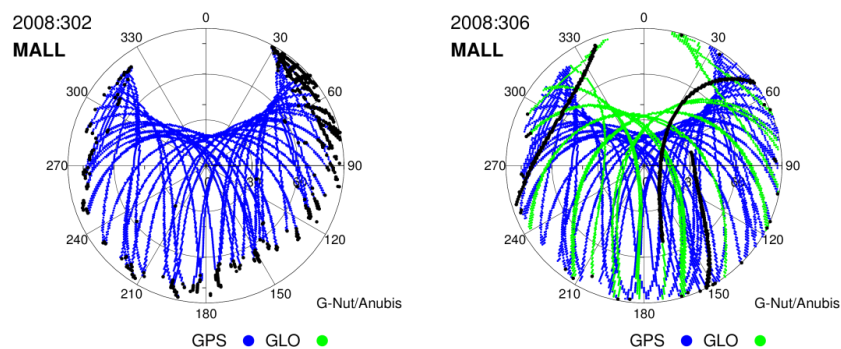


Figure 9: Sky plots before (left) and after (right) replacing the malfunctioning antenna at the MALL site (Oct 30, 2008).  
 Black dots indicates single-frequency observations available only.